RET Is Constitutively Activated by Novel Tandem Mutations that Alter the Active Site Resulting in Multiple Endocrine Neoplasia Type 2B

Aaron N. Cranston,[1] Cristiana Carniti,[3] Kim Oakhill,[2] Elzbieta Radzio-Andzelm,[5] Eric A. Stone,[6] Andrew S. McCallion,[7] Shirley Hodgson,[8] Sue Clarke,[9] Piera Mondellini,[3] Jean Leyland,[1] Marco A. Pierotti,[3,4] Joanne Whittaker,[2] Susan S. Taylor,[5] Italia Bongarzone,[3] and Bruce A.J. Ponder[1]

[1]Cancer Research UK Department of Oncology, Cambridge Institute for Medical Research, University of Cambridge; [2]Department of Medical Genetics, Addenbrooke's Hospital, Cambridge, United Kingdom; [3]Department of Experimental Oncology, Istituto Nazionale per lo Studio e la Cura dei Tumori; [4]The FIRC Institute of Molecular Oncology Foundation, Milan, Italy; [5]Department of Chemistry and Biochemistry, Howard Hughes Medical Institute, University of California, San Diego, La Jolla, California; [6]Department of Statistics and Bioinformatics Research Center, North Carolina State University, Raleigh, North Carolina; [7]McKusick-Nathans Institute for Genetic Medicine, Johns Hopkins University School of Medicine, Baltimore, Maryland; [8]Division of Medical and Molecular Genetics, Guys' Tower, Guys' Hospital; and [9]Department of Nuclear Medicine, Guys' Hospital, London, United Kingdom

Abstract

Constitutive activation of the RET receptor tyrosine kinase underlies the genesis and progression of multiple endocrine neoplasia type 2 (MEN 2), a dominantly inherited cancer predisposition. Importantly, although kinase activation represents a common theme in neoplasias, not all activating mutations are functionally equivalent. Consistent with this, we ascertained a patient with classical features of MEN 2B, but lacking either of the classical mutations in *RET* (M918T or A883F). Instead, the patient harbors a novel pair of germ line missense mutations in *cis* at codons 804 and 805. We evaluated the potential physiochemical effects of these substitutions *in silico*, predicting both to be moderately deleterious in isolation, but severely deleterious in combination. Consistent with this postulate, we show that the identified tandem mutations (V804M/E805K) are biologically active, transforming cells in culture and that their transforming capacity in combination is distinctly synergistic. Furthermore, the V804M/E805K tandem lesion confers resistance to the small molecule receptor tyrosine kinase inhibitor, PP1, suggesting a mode of action distinct from that known for classical MEN 2B mutations. To address this question, we used homology molecular modeling *in silico* to model the active site of RET. We predict that RET804 constitutes a critical gatekeeper residue that, when mutated in combination with RET805, induces a conformational change in the hinge region that locks the active site in a position permissive for ATP hydrolysis. Our findings have implications both in the clinic and in the successful development of novel kinase-targeted anticancer drugs. (Cancer Res 2006; 66(20): 10179-87)

Introduction

Inappropriate activation of receptor tyrosine kinases (RTK) is central to the development and progression of many human neoplastic diseases. One RTK implicated in a series of cancers is RET, a 120-kDa membrane-spanning receptor that transduces signals through multiple intracellular pathways upon activation by the glial cell line–derived neurotrophic factor (GDNF) family of ligands, and in complex with the glycosyl phosphatidyl inositol–anchored glial cell–derived neurotrophic factor family receptor-α coreceptors. RET is expressed at various stages of development and, in the adult, in cell populations derived from the branchial arches, including the parathyroid; from the neural crest, including the brain, parasympathetic and sympathetic ganglia, thyroid C-cells, adrenal medulla, and enteric ganglia; and in the urogenital system (1), and mediates signals proposed to influence cell proliferation, differentiation, migration, and apoptosis (2–6).

RET (*re*-arranged during *t*ransfection), was originally identified as a proto-oncogene in a classic cell transformation study (7, 8), and then later in a proportion of papillary thyroid carcinomas (9). The gene comprises 21 exons encompassing approximately 52 kb of genomic DNA on human chromosome 10q11.2 and generates a transcript that is subject to alternative splicing at both the amino and carboxyl termini, resulting in multiple isoforms. The largest of these encodes a 1,114-residue protein possessing 51 COOH-terminal residues (RET51), whereas the COOH-terminal of the short isoform comprises nine amino acids (RET9; 1,072 aa). Constitutive activating mutations in the *RET* gene were subsequently identified in patients with a dominantly inherited cancer syndrome called multiple endocrine neoplasia type 2 (MEN 2; OMIM 162300 and 171400; refs. 10–12).

MEN 2 is characterized by medullary thyroid carcinoma (MTC) with or without pheochromocytoma and hyperparathyroidism and is subclassified as either (*a*) familial medullary thyroid carcinoma (FMTC), where MTC is the sole indicator of disease; (*b*) type 2A (MEN 2A), where, in addition to MTC, pheochromocytomas and/or hyperparathyroidism associate, albeit with incomplete penetrance; or (*c*) type 2B (MEN 2B), in which MTC is accompanied by developmental abnormalities such as a marfanoid habitus, intestinal dysfunction and ganglioneuromas, thickening of the corneal nerves, neuromas of the lips, tongue, and conjunctiva, and skeletal abnormalities typified by a tall slender physique (5, 13, 14).

Almost all of the MEN 2-causative germ line mutations identified in *RET* are missense mutations concentrated in a small fraction of the open reading frame. Mutations in patients with MEN 2A exclusively affect just five cysteine residues in the extracellular domain (15). Mutation of any one of these cysteines creates an unpaired residue, which can dimerize with another mutant RET

Requests for reprints: Aaron N. Cranston, Cancer Research UK Department of Oncology, Cambridge Institute for Medical Research, University of Cambridge, Hills Road, Cambridge, CB2 2XY, United Kingdom. Phone: 44-1223-336900; Fax: 44-1223-336902; E-mail: aaron.cranston@ntlworld.com.

doi:10.1158/0008-5472.CAN-06-0884

molecule via an illegitimate disulfide bond resulting in constitutive activation of the signaling pathway.

However, the more aggressive MEN 2B subtype is caused exclusively by germ line mutations in the intracellular tyrosine kinase domain of RET (13–17). Almost all (~95%) of the *RET* mutations in MEN 2B are confined to a single amino acid in the intracellular region, $Met^{918}Thr$ (12, 18–20). This residue lies within the substrate-binding pocket of the RET tyrosine kinase and substitution by threonine is thought to alter the substrate specificity of the kinase (21, 22). We (23) and others (24) have previously identified a germ line dinucleotide mutation at codon 883 (A883F) in patients with MEN 2B lacking the M918T mutation, suggesting that MEN 2B could be caused by *RET* mutations other than M918T. This possibility was further strengthened when a combination of two germ line missense mutations *in cis* at valine 804 and tyrosine 806 was reported in a single patient with MEN 2B-like clinical presentation but without either the M918T or A883F mutations (25). These mutations were then shown to be transforming (26). Subsequently, germ line missense mutations at valine 804 and serine 904 were shown to cosegregate with MTC and mucosal neurilemomas in a family with MEN 2B (27). Interestingly, mutation of codon 805 either singly or in combination with codon 804 has not been reported. Furthermore, mutation of valine 804 also characterizes FMTC cases (28) but, until now, the mechanism by which this mutation activates RET was unknown.

Here, we propose a new mechanism by which novel tandem mutations in the tyrosine kinase domain of RET activate this classical RTK. Mutation of valine 804 and glutamate 805 in tandem affects the hinging motion of the kinase lobes, thereby altering the active site and triggering unsolicited activation of a signaling pathway causing the cancer syndrome MEN 2B. This mechanism is distinct from previously reported activating mutations in *RET* and MEN 2.

Materials and Methods

Mutation detection. Genomic DNA extracted from the proband's peripheral blood was analyzed for mutations in exons 10 to 16 of *RET* by DNA sequencing. Blood from her children, sister, and mother were also analyzed; paternal tissue was not available. Sequencing was done in the forward and reverse direction using the BigDye Terminator cycle sequencing kit (Applied Biosystems, Foster City, CA).

Physicochemical conservation and mutational tolerance. We quantified the physicochemical changes in mutant RET proteins against evolutionary variation using multivariate analysis of protein polymorphism (MAPP, see ref. 29). MAPP uses a multiple sequence alignment of protein orthologs to estimate the physicochemical constraints acting on the amino acids observed at each homologous position. The fitness of a substituted protein can then be predicted by a score quantifying the degree to which its amino acid sequence violates these estimated constraints. For this study, the MAPP scores of each substituted variant were calculated as in ref. 30, using the published alignment of human RET with its 11 orthologs (30). Following ref. 29, we obtained conservative P values for each score by comparing one-thirteenth its square to an $F_{6,6}$ distribution (29, 30). To obtain a composite score for tandem substitutions in *cis*, we summed the squared MAPP scores of each substitution and took the square root of the result. We obtained a conservative P value for each composite score by comparing one-thirteenth of its square to the convolution of two $F_{6,6}$ distributions.

Site-directed mutagenesis. Mutations were introduced into both the short (RET9) and long (RET51) 3′-splice isoforms of the human *RET* cDNA in the plasmid, pRCCMV, using the QuikChange site-directed mutagenesis kit (Stratagene, La Jolla, CA).

Cell lines. Cell lines were maintained in DMEM supplemented with 10% Colorado calf serum (Celbio, Italy). Cells were grown at 37°C in 10% CO_2/90% air.

***In vitro* focus formation, kinase, and PP1 inhibitor assays.** The expression constructs were transfected into mouse fibroblast NIH-3T3 cells and their ability to transform assayed as previously described (31). Growth factor stimulation was achieved by adding either GDNF or neurturin (10 ng/μL) to the growth medium. Transformed foci were counted after 2 to 3 weeks and RET expression and phosphorylation checked for each cell line. PP1 inhibitor [4-amino-5-(4-methylphenyl)-7-(-*t*-butyl)-pyrazolo-D-3,4-pyrimidine; BioMol Research Laboratories, Plymouth Meeting, PA], was dissolved in DMSO and diluted into the culture medium to 1 μmol/L for 12 hours. Cells were lysed as reported (32), immunoprecipitated with anti-RET polyclonal antibody (C-19; Santa Cruz Biotechnology, Santa Cruz, CA), and protein concentration estimated by a modified Bradford assay (Bio-Rad, Munich, Germany). Immune complexes were separated by SDS-PAGE and immunoblotted using a mouse antiphosphotyrosine antibody (4G10; Upstate Biotechnology Inc., Lake Placid, NY).

***In silico* homology molecular modeling.** Based on the coordinates of the active insulin receptor kinase (IRK; ref. 33), a homology model of RET was constructed using the Homology module in Insight II, a homology molecular modeling software program (Accelrys, Inc., San Diego, CA). In this model (residues 713-1018), Val^{804} and Glu^{805} correspond to residues Met^{1076} and Glu^{1077} in IRK, and Met^{120} and Glu^{121} in protein kinase A (PKA).

Results

Clinical history of the patient. The female proband (Fig. 1*A*) presented at 50 years of age with diarrhea and was diagnosed with endometrial adenocarcinoma. She was also found to have a clear cell carcinoma of one ovary, and endometrial cancer that had spread to the contralateral ovary. She was treated by hysterectomy and bilateral oophorectomy followed by radiotherapy. On follow-up 10 months later, she had a persistently increased CEA level and an 18FDG PET scan showed uptake in the thyroid and adrenals. Subsequently, she was also found to have a thyroid mass, with an increased blood calcitonin level. A fine-needle aspirate showed medullary carcinoma of the thyroid, and a methyliodobenzylguanidine scan preoperatively showed bilateral pheochromocytomas, confirmed biochemically by increased urinary catecholamines and by histology. She was treated by bilateral laparoscopic adrenalectomies, during which a liver biopsy showed metastatic medullary cell thyroid carcinoma. Total thyroidectomy was done and histology confirmed multifocal medullary thyroid carcinoma invading into local nerve and muscle. Consistent with these observations, the patient possessed a marfanoid habitus with a typical MEN 2B facial appearance. She had prominent nodules on her lips and tongue (Fig. 1*A*), a small pigmented lesion on the skin of her right calf and ophthalmologic examination revealed thickening of the corneal nerves, all features of the MEN 2B syndrome. Apart from diverticulitis, she has remained well 4 years later. There was no family history of cancer except for her father, who died of carcinoma of the bladder at 60 years of age.

The V804M/E805K tandem mutations are present in *cis* and cause MEN 2B. DNA sequencing revealed the presence of two missense mutations in exon 14 of *RET*. At codon 804, methionine was substituted for valine (GTG → ATG), whereas at codon 805, lysine was substituted for glutamate (CAG → AAG). The tandem V804M/E805K mutations lie within the RET tyrosine kinase domain (Fig. 1*B*). No further mutations were detected in exons 10 to 16. Although DNA from the proband's father was not available for analysis, neither mutation was found in the proband's children

or her mother, suggesting that the tandem mutations were present on the same allele.

To confirm this, a region spanning exon 14 was amplified from genomic DNA by PCR, subcloned and analyzed by sequencing and digestion with *Rca*I (*Bsp*HI). DNA sequencing of the amplicon revealed the presence of both mutations in *cis* (Fig. 1*C*). *Rca*I restriction analysis of the amplicon produced products of 230 and 73 bp (data not shown), further confirming that both mutations were present in the *cis* configuration; mutation of codons 804 or 805 alone is not sufficient to create the *Rca*I recognition site.

Correlating tandem mutations with observed phenotypes. The phenotypic effect of disease-causing changes in the RET protein sequence varies inversely with the degree to which the physicochemical properties of the substituted amino acid are conserved throughout vertebrate evolution (30). We reasoned that the effect of tandem substitutions in RET, including $RET^{V804M/E805K}$, should similarly correlate with aggregate physicochemical change. To substantiate this, we identified, from the literature, four additional reports of tandem mutations in RET: (*a*) $RET^{V804M/Y806C}$ (25) and (*b*) $RET^{V804M/S904C}$ (27) in MEN 2B, and (*c*) $RET^{V804M/V778I}$ (34) and (*d*) $RET^{V804M/R844L}$ (35) in FMTC. We then extended the physicochemical conservation metric used in the previous study (MAPP, see Materials and Methods) to accommodate multiple substitutions in *cis*. Insofar as MEN 2B is a more severe phenotype than FMTC, we expected the tandem mutations identified in FMTC to be less radical than their MEN 2B counterparts in terms of aggregate physicochemical change from wild-type. This expectation was strongly confirmed (Fig. 1*D*), and we proceeded to predict the effect of $RET^{V804M/E805K}$ using the same physicochemical criteria. Consistent with our hypothesis, the physicochemical change in $RET^{V804M/E805K}$ is consistent with the other MEN 2B cases and is greater than that observed in FMTC (Fig. 1*D*).

We next sought physicochemical context for the synergy between V804M and E805K in transforming potential. To accomplish this, we scored $RET^{V804M/E805K}$ against its constituent single substitution TK mutants, V804M and E805K, normalizing the tandem mutant appropriately for comparison (see Materials and Methods). The aggregate physicochemical change in the tandem mutant, as quantified by its MAPP score (31.56) and associated *P* values (6.5×10^{-4}), suggested a phenotype more severe than that of either RET^{V804M} (score, 24.43; $P = 9.4 \times 10^{-5}$) or RET^{E805K} (score, 19.98; 19.98; $P = 3.0 \times 10^{-4}$). Equating this severity to transforming potential, we then tested these predictions directly on cells in culture.

The V804M/E805K tandem mutations are biologically active and transform cells. The transforming activity of the $RET^{V804M/E805K}$ mutations in both short (RET9) and long (RET51) 3′-splice isoforms (Fig. 1*B*) was assayed by transfecting NIH-3T3 cells in parallel with the wild-type cDNA and with other known

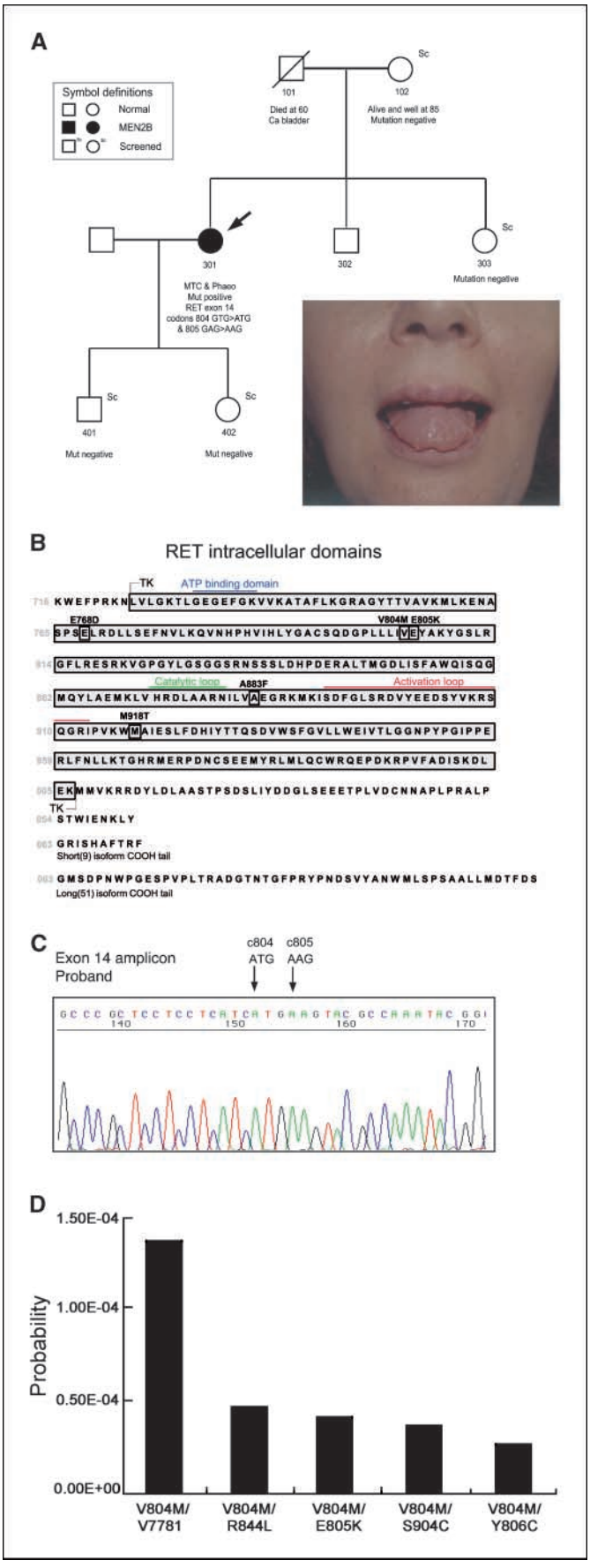

Figure 1. Clinical molecular genetics of the patient. *A,* pedigree of the MEN 2B family (*arrow,* proband); clinical features of MEN 2B (bumpy lips and tongue) in the proband. *B,* the location of the tandem mutations in the RET intracellular TK domain (*circled*). *C,* DNA sequencing of one allele of the proband's subcloned DNA revealed the presence of tandem missense mutations at codons 804 and 805 in exon 14 of the *RET* gene. *D,* MAPP-based *P* values of substituted RET variants quantify their predicted phenotypic effect. Tandem mutations identified in FMTC are less radical than those identified in MEN 2B. *Columns*, *P* values of five RET tandem mutants, from left to right: $RET^{V804M/V778I}$ and $RET^{V804M/R844L}$, identified in FMTC, and $RET^{V804M/E805K}$, $RET^{V804M/S904C}$, and $RET^{V804M/Y806C}$, identified in MEN 2B.

activating mutations (i.e., E768D, V804M, A883F, and M918T). In order to quantify the transforming potential of these mutations, we assayed the number of focus-forming units per microgram of DNA transfected, either in the absence or presence of chronic growth factor stimulation. We used the ligands, GDNF and neurturin, because experiments in our lab indicated that the receptors for these particular growth factors were expressed in NIH-3T3 cells.[10]

The transforming potential of the kinase mutants in the RET 3′-short isoform is very low in the absence of either ligand (Fig. 2*A*). Upon chronic stimulation with either GDNF or neurturin, each of the mutations, with the exception of E805K, displayed increased transforming activity (Fig. 2*A*). In contrast, the E805K mutation in the short isoform is barely stimulated above a basal level of activity by the addition of either ligand (Fig. 2*A*).

The tandem V804M/E805K mutations in the long isoform, examined in the absence of ligand stimulation, induced 42 transformed foci per microgram of DNA transfected. This is about half the activity of the classical MEN 2B mutations, A883F and M918T (Fig. 2*B*). Moreover, the transforming potential of the tandem mutations is higher than the sum of the individual mutations alone (V804M/E805K, V804M, and E805K; 42 foci versus 9 versus 8, respectively), indicating that there is synergy when the mutations are in combination. Importantly, the transforming potential of the other TK mutants tested (E768D, V804M, and E805K) is between 8- and 16-fold lower than that of the RET^{A883F} mutation and between 10- and 19-fold lower than that of the RET^{M918T} mutation on the same isoform, confirming that these kinase mutants are only capable of conferring weak oncogenic potential to RET (Fig. 2*B*). With the exception of the A883F, M918T, and tandem V804M/E805K mutations, the transforming activity of the kinase mutations is further increased by the addition of either GDNF or neurturin. Thus, the transforming activity of the tandem V804M/E805K mutations or classical MEN 2B mutations (A883F and M918T) is growth factor stimulation–independent.

The PP1 inhibitor has specific effects on mutant RET oncoprotein transformation. The small molecular weight pyrazolo-pyrimidine inhibitor, PP1, abrogates the morphologic changes induced by the expression of RETMEN 2A and RETMEN 2B oncoproteins in NIH-3T3 cells and induced dephosphorylation of these mutant proteins (36). To determine whether the V804M, E805K, and V804M/E805K-transformed cells would respond similarly, we cultured each in the presence of PP1.

Consistent with the finding for RETMEN 2A and RETMEN 2B oncoproteins, when examined by phase-contrast microscopy, the morphology of the cells harboring the E805K mutation reverted upon PP1 treatment. In contrast, no morphologic reversion was observed for the cells harboring either the V804M or the tandem mutations (Fig. 3*A*).

To assess the effects of PP1 on RET phosphorylation, cells were incubated in the absence or presence of PP1 prior to lysis. RET tyrosine-phosphorylated proteins were analyzed by Western blotting with anti-pTyr antibodies. Consistent with cellular morphology data, PP1 dramatically reduced the amount of phosphorylated RET in cultures harboring the E805K mutation; PP1 treatment was ineffective in reducing phosphorylation in RET proteins harboring the V804M or tandem V804M/E805K mutations (Fig. 3*B*).

[10] Unpublished results.

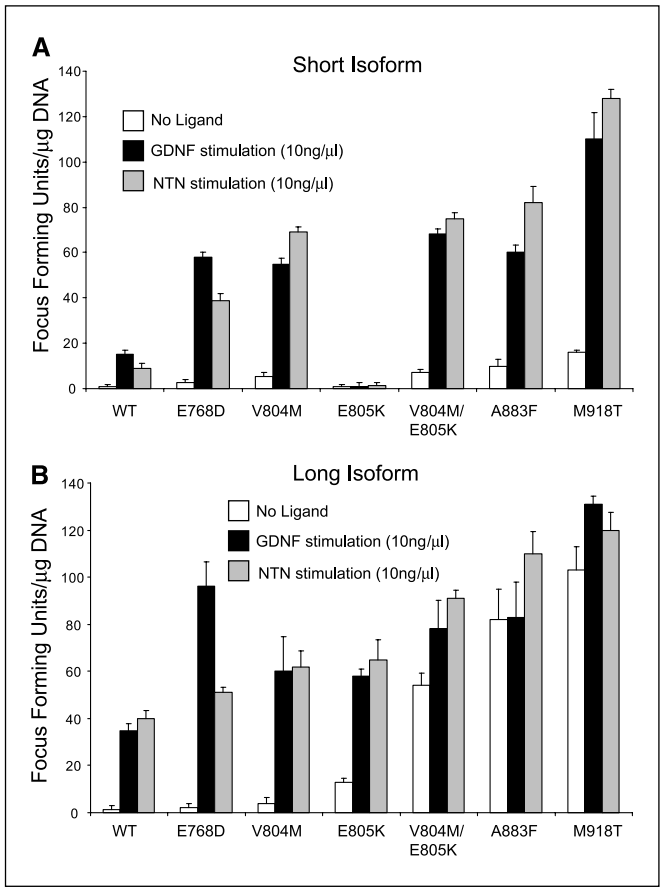

Figure 2. Transforming activity of the RET mutants. *Columns,* transformation potential of V804M, E805K, or the V804M/E805K mutations in a *RET* cDNA encoding the short isoform (*A*), or the long isoform (*B*). Other known *RET* gain-of-function mutations were assayed for comparison. *White columns,* no growth factor ligand present; *black columns,* GDNF added to the culture medium at 10 ng/μL; *gray columns,* neurturin added to the culture medium at 10 ng/μL.

***In silico* structural modeling predicts the V804M/E805K tandem mutations alter the RET kinase hinge region and reposition the active site cleft such that it is constitutively active.** In our homology molecular model of the RET kinase, based on the structure of active IRK (33), and a sequence alignment with IRK (37) and PKA (Fig. 4), the kinase domain starts at position 713 and ends at position 1018. Residues Val^{804} and Glu^{805} correspond to Met^{1076} and Glu^{1077} in IRK, and Met^{120} and Glu^{121} in PKA, respectively.

The model reveals a two-lobed structure typical of tyrosine kinase catalytic domains, in which Val^{804} and Glu^{805} are located at the junction of the fifth β-strand and the linker segment, which joins the small and large lobes of the kinase core (Fig. 5*A* and *B*). This linker is the major component of the hinge mechanism that facilitates the opening and closing of the catalytic cleft (38, 39), hence, mutation of this region could affect the kinase hinging mechanism. It also forms a critical part of the adenine binding pocket, in which the backbone carbonyl hydrogen of Glu^{805} bonds to ATP (via the N-hydrogen of the 6-amino adenine ring in ATP). In our structural model, Glu^{805} lies in close proximity to Lys^{889} in the eighth β-strand at distances of R = 2.9 Å and R = 3.3 Å. This interaction is conserved in the IRK in which Glu^{1077} (corresponding to Glu^{805} in the RET model) interacts with Lys^{1147} (corresponding

to Lys[889] in RET). There is a similar interaction in PKA albeit at longer distances: Glu[121] interacts with Gln[181] (corresponding to Lys[889] in RET) at R = 3.6 Å. In PKA, the closest positively charged residue is Lys[105] at the beginning of the fourth β-strand at R = 3.9 Å. The E805K mutation changes the character of the amino acid at this position, conferring a positive charge and thus creating charge repulsion with Lys[889]. This newly created Lys[805] has the potential to interact with another nearby negatively charged residue, the closest candidate being Glu[884], positioned between the seventh and eighth β-strands. The reduction or inhibition of activity conferred by this mutation in the shorter RET isoform could thus be due to charge repulsion between Lys[805] and Lys[889] and/or formation of an inappropriate ion pair that locks the enzyme into an inactive conformation. As this site is close to the hinge and also contributes to the adenine binding pocket, it is likely to be critical for generating an active enzyme.

In contrast to Glu[805], Val[804] is hydrophobic and is part of a hydrophobic nodule that is comprised of residues from different parts of the protein: Ile[788] (loop between C helix and fourth β-strand), Ala[756] (third β-strand), Leu[779] (C helix), Leu[790] (fourth β-strand), and Leu[802] (fifth β-strand). This hydrophobic pocket is conserved in IRK (Val[1060], Val[1010], Met[1051], Leu[1062], and Val[1074]) and in PKA (Val[104], Val[57], Leu[95], Leu[106], and Met[118]) and may be important for the hinging motions discussed above. In fact, this hydrophobic pocket appears to be a conserved feature of most, if not all, protein kinases. In the IRK structure, the residue

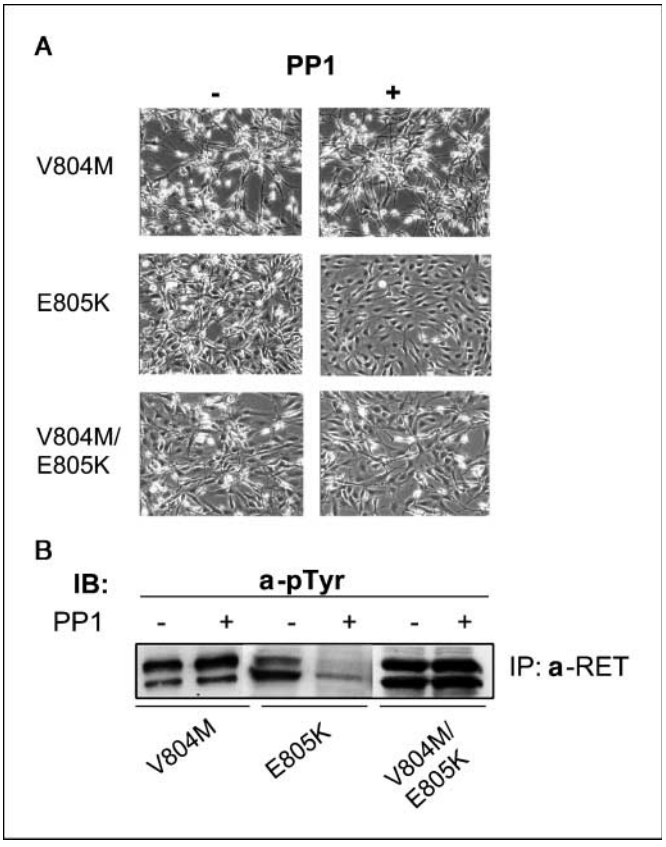

Figure 3. Effects of PP1 on RET^{V804M}-, RET^{E805K}-, and RET$^{V804M/E805K}$-transformed cells. *A,* PP1 reverts the transformed morphology of RET^{E805K}, but not that of RET^{V804M} and RET$^{V804M/E805K}$ mutant NIH-3T3 fibroblasts. *B,* PP1 induces the dephosphorylation of RET^{E805K} but not RET^{V804M} or RET$^{V804M/E805K}$. Anti-RET immunocomplexes (*IP*) for RET^{V804M}-, RET^{E805K}-, and RET$^{V804M/E805K}$-expressing fibroblasts.

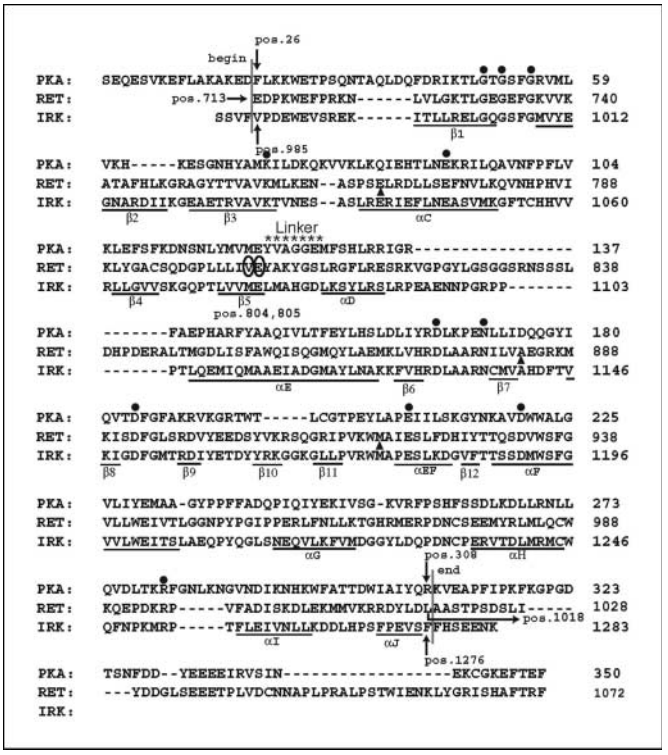

Figure 4. Homology alignment of the RET tyrosine kinase domain. Our model is based on the active IRK and the RET kinase starts at position 713 and ends at position 1018. Tandem V804M/E805K mutations (*encircled*); conserved residues (●); mutated residues (▲). The alignment for RET and IRK kinases was taken from ref. 33. PKA was aligned to RET based on the alignment from PileUp multiple sequence alignment program from Genetic Computer Group Wisconsin Package Programs.

corresponding to Val[804] is actually a methionine (Met[1076]), and this methionine interacts with the hydrophobic pocket described above. Following mutation, the interactions of V804M are similar with residues Ile[788], Ala[756], Leu[779], Leu[790], and Leu[802]. Even though the methionine residue is larger than the valine, it seems to fit well in this hydrophobic environment. However, the longer methionine does reach better to the COOH terminus of the C helix. Indeed, both residues, 804 and 805, are close to the COOH terminus of the C helix, and it is this helix that must be aligned properly in the active enzyme. Correct positioning of the C helix is an essential requirement of the activation process for most protein kinases. The evolutionary physicochemical and steric constraints evident within this region strongly suggest a critical role for this configuration and a significantly deleterious outcome to mutations therein.

Discussion

Clearly, the ability to discriminate points along the spectrum between neutral and deleterious amino acid substitutions in the genes of patients remains a significant challenge to our understanding of disease mechanisms and consequently to patient care. Importantly, although so-called classical mutations can teach us much about the pathogenesis of disease, it is the exceptions to a rule that are frequently responsible for expanding the boundaries of our understanding. We have identified novel missense mutations affecting codons 804 and 805 on the same allele of the *RET* proto-oncogene. We report detailed evaluation of these tandem

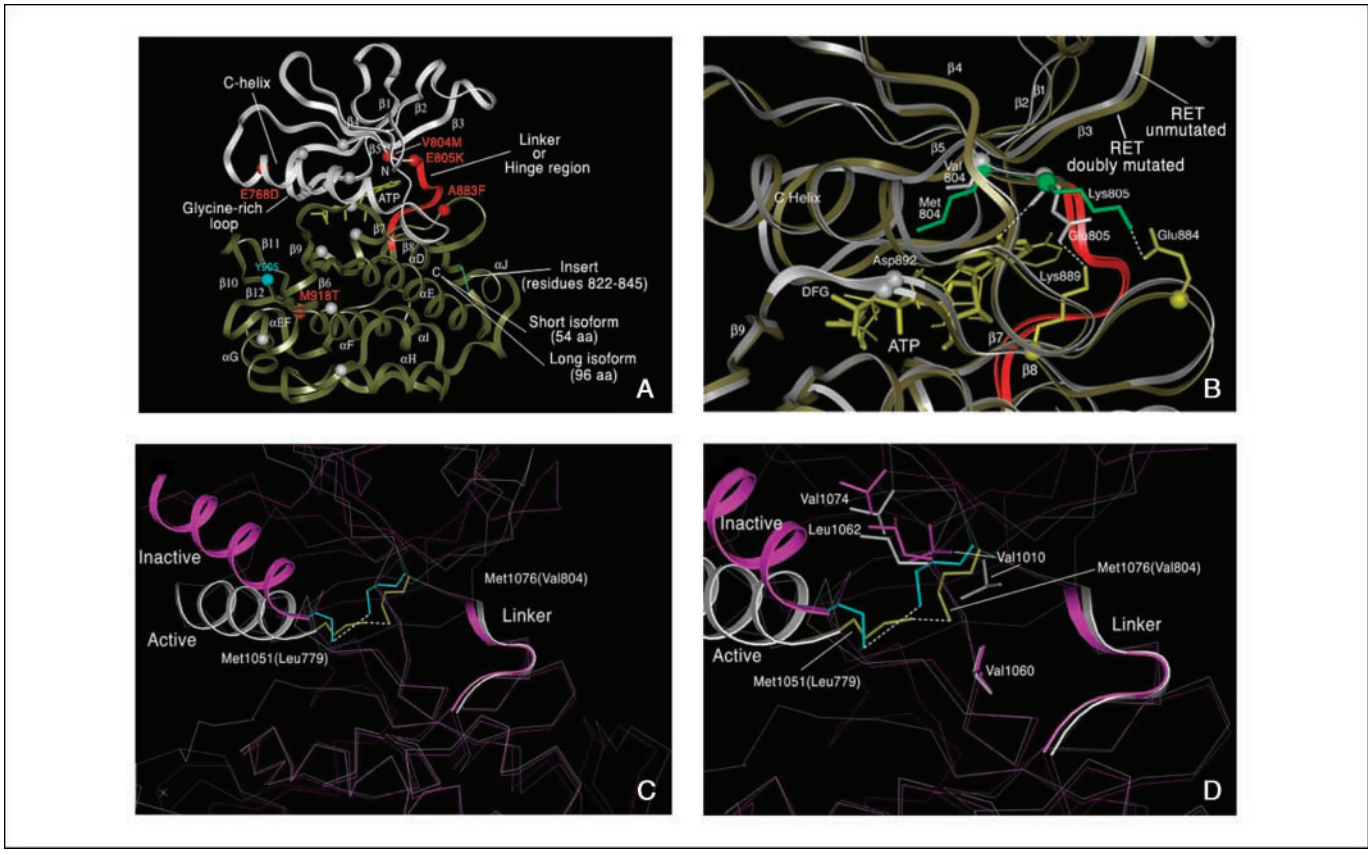

Figure 5. Homology molecular modeling of the RET tyrosine kinase domain. *A,* ribbon diagram of the wild-type RET tyrosine kinase domain (residues 713-1018). Small lobe (*white*); large lobe (*bronze*); the linker, or hinge, region (residues 806-811; *red*); and the insert region (*green*). The conserved kinase residues (Gly^{731}, Gly^{733}, Gly^{736}, Lys^{758}, Glu^{775}, Asp^{874}, Asn^{879}, Asp^{892}, Asp^{933}, Glu^{921}, and Arg^{995}; *gray balls* representing the α-carbon atoms). The mutated residues E768D, V804M, E805K, A883F, and M918T (*red balls*). The Tyr^{905} residue, which is to be phosphorylated (*turquoise ball*). *B,* two ribbon structure models are compared in the tandem mutation region: the wild-type model (*gray*) and the tandem mutated model (*bronze*). Val^{804} and Glu^{805} (*gray*), the mutated residues Met^{804} and Lys^{805} (*green*). Lys^{889}, which potentially interacts with Glu^{805} in the wild-type model, and Glu^{884} in the tandem mutated structure, which possibly interacts with Lys^{805} (*yellow*). The ATP in both structures (*thick yellow line,* wild-type structure; *thin yellow line,* tandem mutated structure). *Red,* the linker, or hinge, region (residues 806-811); *white,* the DFG region (residues 892-894). *C,* superimposition of the α-carbon backbones of the inactive (*pink*) and active (*white*) IRK. *Ribbons,* the α-helix C (residues 1038-1052) and hinge regions (residues 1078-1083). The side chains of Met^{1051} and Met^{1076} in the inactive IRK (*turquoise*) and in the active IRK (*yellow*). *Dashed line,* the distances between Met^{1051} and Met^{1076}. *D,* in the enlargement of (*C*), the hydrophobic residues Val^{1074}, Leu^{1062}, Val^{1010}, and Val^{1060} are added to both structures.

mutations, elucidating their biological characteristics both in isolation and in combination and propose a novel mechanism by which they trigger the activation of RET resulting in MEN 2B.

To date, germ line point mutations in exon 14 leading to substitution of RET Val^{804} by either leucine or methionine have been reported in patients with sporadic MTC or FMTC (28, 40–44). However, the V804M mutation has only been reported in patients with MEN 2B when it is present on the same *RET* allele with a missense mutation at either codon 806 (25) or codon 904 (27). Neither germ line nor somatic mutations of codon 805 have been reported previously in MEN 2 or FMTC. Notwithstanding the possibility that the mutations could have arisen *de novo* in previous generations, we proposed that the pairing of V804M and E805K may exemplify a novel class of *RET* mutations, whose tumorigenic activity in combination is uncharacteristically severe. We therefore set out to evaluate the effect of these novel tandem mutations on the MEN 2 disease phenotype.

Given that the phenotypic effect of disease-causing substitutions in the RET protein sequence varies inversely with physicochemical and evolutionary constraint (30), we posited, that the effect of the tandem mutations in *RET* correlates strongly with the aggregate physicochemical change. Furthermore, insofar as MEN 2B is a more severe phenotype than FMTC, we showed that the physicochemical consequences of $RET^{V804M/E805K}$ more closely resemble the other MEN 2B cases than those observed in FMTC.

To test our hypotheses directly, we did classic transformation studies introducing the mutations into the short (RET9) and long (RET51) splice isoforms, producing data that strongly supported our expectations. For example, in the long isoform, the tandem $RET^{V804M/E805K}$ mutations displayed a level of transforming activity greater than that of either mutation alone, and greater than the sum of its parts, indicating that this combination of mutations is highly synergistic. This transforming activity is also stronger than that of two weakly activating RET mutations (E768D and V804M), but not quite as potent as the highly activating mutations, A883F and M918T, which are historically associated with MEN 2B; this may also explain the relatively late age-of-onset of MEN 2B in this patient. However, like the A883F and M918T mutations, the level of activation of V804M/E805K is not enhanced greatly in the presence of ligand. This suggests that, at least in the long isoform, these mutant receptors do not need to dimerize to achieve activation.

To address the mechanism by which the tandem V804M/E805K mutations activate RET, we did comparative homology molecular modeling experiments in which we generated a structural model of

the RET tyrosine kinase domain (Fig. 5*A*). The model clearly predicts a classical two-lobed structure with a relatively open ATP binding site (Fig. 5*A*). The tandem V804M/E805K mutations are located at a critical "hub" site that lies at the major hinge point between the small and large kinase lobes, which form the cytoplasmic TK catalytic domains (Fig. 5*A* and *B*). Our results show that mutations in this region have the potential to be activating or inhibiting. Several of the major elements of secondary structure converge at this point, therefore, small changes could be propagated over long distances. Val^{804} and Glu^{805} contribute in quite different ways to this hinge region.

Val^{804} contributes to a hydrophobic region, and its replacement by methionine introduces a bulkier group but does not change the properties of the side chain. Most likely, it helps to correctly position the α-helix C for catalysis. One can appreciate the crucial position of this residue and its relationship to the C helix when inactive IRK is compared with activated IRK (Fig. 5*C* and *D*). Additionally, the V804M mutation is activating in both isoforms.

Not only is Glu^{805} located at the junction of the fifth β-strand and the linker segment (residues 806-811), which joins the small and large kinase lobes, but it also contributes to the ATP binding pocket. Specifically, Glu^{805} hydrogen bonds to the adenine ring in ATP. A similar interaction exists when the active IRK and PKA structures are compared (33). In fact, this interaction is conserved in most protein kinases. Mutation of this Glu^{805} to lysine changes the electrostatic properties of the region. Lys^{889}, which seems to interact with Glu^{805} in our wild-type RET model, an interaction that is also conserved in IRK, lies in the eighth β-strand preceding the conserved DFG loop (also termed the magnesium positioning loop). When the ionic interaction between Lys^{889} and Glu^{805} is broken following mutation, not only would there be charge repulsion between Lys^{805} and Lys^{889}, but Lys^{889} does not have another negatively charged residue with which to bind. This could distort the position of the DFG loop. Clearly then, this region is important for activation, most likely for correctly orienting the C helix.

The underlying mechanism seems to be at least partly dependent on the length of the carboxyl-terminal tail because transforming activity is much higher in the long isoform than in the short isoform, suggesting that the longer carboxyl-terminal tail might directly or indirectly interface with this region. Furthermore, consistent with a mechanism in which the receptor does not need to dimerize to become constitutively activated, the tandem mutations are highly activating even in the absence of exogenous growth factor stimulation. This is consistent with a prediction that the primary role of dimerization is to stabilize an inhibited form of RET rather than to specifically stabilize an active conformation.

We synthesized these results into a working model illustrating the novel hinging mechanism by which the newly identified tandem mutations could constitutively activate the RET kinase domain in the absence of growth factor stimulation (Fig. 6). Mutation of V804 and E805 in the critical kinase hinge region has a 2-fold effect: first, it results in a conformational change, which closes the catalytic cleft; and second, this in turn correctly repositions the C helix and DFG residues, thereby facilitating catalysis. The outcome, release of the kinase from its normal autoinhibited state (45), which can occur in the absence of a growth factor signal, is orientation of the active site cleft into a more optimal position for the binding of ATP and subsequent autophosphorylation of the catalytic tyrosine (Y905). Consequently, the mutant monomeric $RET^{V804M/E805K}$ kinase is "switched on" in the absence of exogenous growth factor signals.

Our data suggest that the RET kinase domain harbors at least two regions in which substitutions might maximally affect protein function. The common M918T mutation is clearly in the first "hot-spot" region, the peptide binding site, but this residue is also very important for activity. Indeed, in the activation loop of Ser/Thr kinases, this threonine is absolutely essential for activity (46), but it does not determine substrate specificity. Equally, $RET^{V804M/E805K}$ and the other MEN 2B mutation, RET^{A833F}, reside around the hinge region, and mutation of this second mutation hot-spot region most likely influences conformational states. The hinge region forms part of the ATP binding pocket for the adenine ring and these mutations seem to shift the enzyme into an active conformation, which is then independent of GDNF. Thus, they release an inhibition that is imposed by the longer COOH-terminal tail in the absence of ligand.

The results obtained with the small molecule TK inhibitor, PP1, underscore the importance of understanding the biochemical events that underlie the activation of protein kinases in cancer. Although effective against the E805K mutation, RET/PTC3—a fusion protein of the RET TK domain with the RFG gene (47, 48), and the Src and PDGFR kinases (49), the kinase inhibitor PP1 did not inhibit $RET^{V804M/E805K}$ or RET^{V804M}. Recently, disease-associated mutations at valine 804 conferred resistance to a series of small molecule kinase inhibitors (50). Our homology model data suggests that, in these mutants, the methionine lies closer to PP1 than did the deposed valine. Specifically, we predict that the methionine of codon 804 lies over the methyl-phenyl ring of PP1 in the ATP-binding pocket and that the close proximity of the mutant residue to the inhibitor is sufficient to prevent competitive inhibition of the active site. Consistent with this postulate, we show that differences exist between the mutated (V804M, E805K, and V804M/E805K) and wild-type RET when they are modeled in combination with ATP (data not shown). Overall, ATP is shifted, especially in the V804M and V804M/E805K mutated kinases, when compared with PP1. This indicates that the difference in response to PP1 is due to a mutation-induced difference in the conformation of the ATP-binding site and suggests that PP1 is noncompetitive with ATP for the inhibition of RET^{V804M} and $RET^{V804M/E805K}$, but that it is competitive with ATP for the inhibition of RET^{E805K}. Therefore, PP1 is a mixed competitive inhibitor vis-à-vis the substrate. Although it is possible that residue 768 could hydrolyze ATP, mutation of 768 does not lock the hinge region in an open aspect (data not shown). This could explain why mutation of this particular residue is milder and only found in cases of FMTC.

Crucially, in our model of the RET catalytic subunit, Val^{804} is the "gatekeeper"[11] residue and mutation to methionine makes it unresponsive to small molecule kinase inhibitors. This is also consistent with studies in which protein engineering of the PKA gatekeeper residue, Met^{120} to either alanine or glycine, induced sensitivity to a series of pyrazolo-pyrimidine-based inhibitors (51). We have since shown that this is because PKA can accept the bulky ATP analog inhibitor when the methionine is replaced by alanine.[12] Conversely, mutation of the RET gatekeeper from valine to methionine means that PP1 can no longer fit in the active site.

[11] Gatekeeper—a single active site residue that governs nucleotide substrate specificity.

[12] Unpublished data.

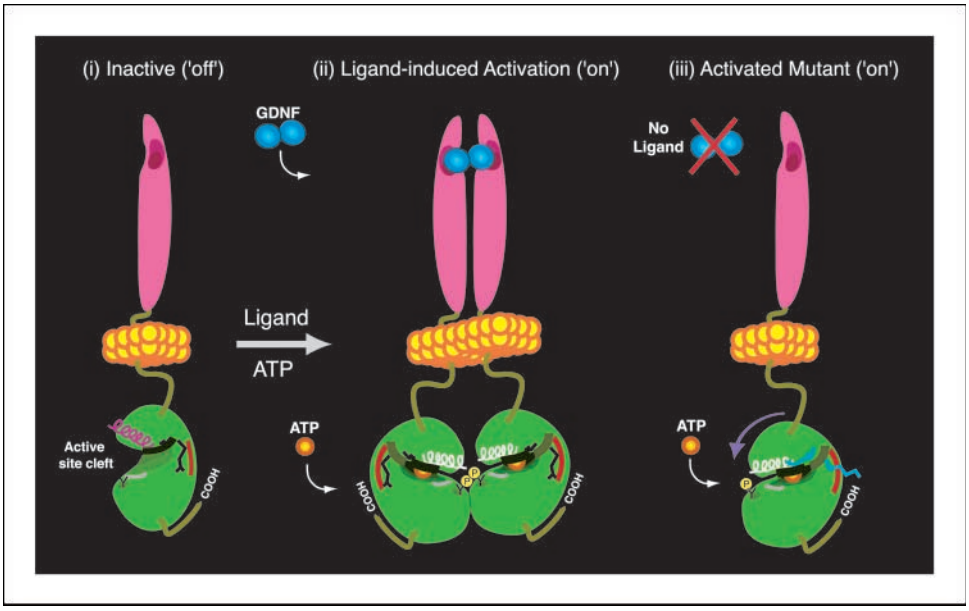

Figure 6. A mechanism for the activation of the RET tyrosine kinase domain by the tandem V804M/E805K mutations. The structure of the kinase is drawn as an interpretation of our homology model as two lobes linked by a hinge region (*red*). The α-helix C (*pink,* inactive kinase; *white,* activated kinase) and DFG conserved sequence (*gray*) are also shown. Val^{804} and Glu^{805} (*black "sticks"*) are replaced by Met^{804} and Lys^{805} (*blue "sticks"*) in the mutated kinase; the change in conformation of the critical hinge region induced by the tandem mutations, such that the orientation of the kinase lobes are made permissive for ATP (*orange*) binding, is represented by the direction of the purple arrow in (*iii*). The catalytic tyrosine (*Y*), phosphorylation events (*P*) and carboxyl-terminal tail are also shown. The inactive RET kinase (*i*) is ordinarily activated by ligand-induced dimerization (*ii*), which induces a conformational change in the NH_2-terminal and COOH-terminal lobes of the tyrosine kinase domain such that the active site cleft is permissive for ATP binding. Note that the orientation of the C helix changes in the activated kinase (*pink to white*) and that the active site cleft is now optimally positioned for binding ATP. However, when present, (*iii*) the tandem V804M/E805K mutations activate the kinase in the absence of ligand by inducing a conformational change in the hinge. With the kinase lobes "locked" in this position, the C helix is favorably positioned for binding ATP in the active site cleft. This facilitates kinase activation and subsequent autophosphorylation of the catalytic tyrosine. The result of the tandem mutations is to switch the kinase into the "on" position despite the absence of ligand. For simplicity, the glycosyl phosphatidyl inositol–linked coreceptors are not shown. *Pink,* cysteine-rich extracellular domain; *blue,* the ligand homodimer; *yellow spheres,* the plasma membrane; *green,* the intracellular kinase domain.

Our data also illuminate the differences between the RET V804M, E805K, and V804M/E805K mutations in response to drug treatment. Therefore, successful extension of kinases as druggable targets for other cancers (52) raises many challenges, including the need for molecular analysis of tumors from patients and the development of specific kinase inhibitors with requisite target specificity. This is further illustrated by Gleevec (Glivec/STI-571/imatinib mesylate), a small molecule inhibitor, which initially showed dramatic clinical value in the treatment of patients with BCR-ABL-positive chronic myeloid leukemia and c-KIT-positive gastrointestinal stromal tumors (53), but in which some tumors were clinically resistant to treatment. Investigation into the mechanism of resistance has shown that this occurs through point mutations in the catalytic sites of the BCR-ABL and c-KIT kinase domains (54). Significantly, the tandem V804M/E805K mutations in RET correspond to the key site that most likely accounts for the specificity of Gleevec. In ABL, the gatekeeper residue is a threonine, which allows Gleevec to bind, whereas the most common mutation found in patients resistant to treatment is a threonine to tyrosine mutation, which sterically blocks Gleevec binding and which is functionally equivalent to the $Val^{804}Met$ mutation in RET.

A fuller understanding of the functional consequence of such *RET* mutations will undoubtedly promote important clinical interventions and should lead to the development of tailored drug therapies for MEN 2-related cancers and its associated sporadic cancers. More broadly, the emerging power of chemical genetics (55), when combined with classical genetic and biochemical data, facilitates a better understanding of protein function and dysfunction.

Acknowledgments

Received 3/9/2006; revised 7/18/2006; accepted 8/4/2006.

Grant support: Cancer Research UK (B.A.J. Ponder), Télethon (I. Bongarzone), U.S. Army Grant AIBS1762 (S.S. Taylor), and March of Dimes (A.S. McCallion).

The costs of publication of this article were defrayed in part by the payment of page charges. This article must therefore be hereby marked *advertisement* in accordance with 18 U.S.C. Section 1734 solely to indicate this fact.

The authors thank the patient and her family for their continued cooperation. B.A.J. Ponder is a Gibb fellow of Cancer Research UK.

References

1. Nakamura T, Ishizaka Y, Nagao M, Hara M, Ishikawa T. Expression of the ret proto-oncogene product in human normal and neoplastic tissues of neural crest origin. J Pathol 1994;172:55–60.
2. Airaksinen MS, Titievsky A, Saarma M. GDNF family neurotrophic factor signaling: four masters, one servant? Mol Cell Neurosci 1999;13:313–25.
3. Saarma M, Sariola H. Other neurotrophic factors: glial cell line-derived neurotrophic factor (GDNF). Microsc Res Tech 1999;45:292–302.
4. Baloh RH, Enomoto H, Johnson EM, Jr., Milbrandt J. The GDNF family ligands and receptors—implications for neural development. Curr Opin Neurobiol 2000;10:103–10.
5. McCallion AS, Chakravarti A. RET and Hirschsprung disease and multiple endocrine neoplasia type 2. In: Epstein C, Erickson R, Wynshaw-Boris A, editors. Inborn errors of development. San Francisco: Oxford University Press; 2004. p. 421–32.
6. Marx SJ. Molecular genetics of multiple endocrine neoplasia types 1 and 2. Nat Rev Cancer 2005;5:367–75.
7. Takahashi M, Ritz J, Cooper GM. Activation of a novel human transforming gene, ret, by DNA rearrangement. Cell 1985;42:581–8.
8. Takahashi M, Cooper GM. ret transforming gene encodes a fusion protein homologous to tyrosine kinases. Mol Cell Biol 1987;7:1378–85.
9. Bongarzone I, Pierotti MA, Monzini N, et al. High frequency of activation of tyrosine kinase oncogenes in

human papillary thyroid carcinoma. Oncogene 1989;4:1457–62.
10. Donis-Keller H, Dou S, Chi D, et al. Mutations in the RET proto-oncogene are associated with MEN 2A and FMTC. Hum Mol Genet 1993;2:851–6.
11. Mulligan LM, Kwok JB, Healey CS, et al. Germ-line mutations of the RET proto-oncogene in multiple endocrine neoplasia type 2A. Nature 1993;363:458–60.
12. Hofstra RM, Landsvater RM, Ceccherini I, et al. A mutation in the RET proto-oncogene associated with multiple endocrine neoplasia type 2B and sporadic medullary thyroid carcinoma. Nature 1994;367:375–6.
13. Ponder BA. The phenotypes associated with ret mutations in the multiple endocrine neoplasia type 2 syndrome. Cancer Res 1999;59:S1736–41.
14. Jhiang SM. The RET proto-oncogene in human cancers. Oncogene 2000;19:5590–7.
15. Mulligan LM, Marsh DJ, Robinson BG, et al. Report of the International RET Mutation Consortium. Genotype-phenotype correlation in multiple endocrine neoplasia type 2. J Intern Med 1995;238:343–6.
16. Santoro M, Carlomagno F, Melillo RM, Billaud M, Vecchio G, Fusco A. Molecular mechanisms of RET activation in human neoplasia. J Endocrinol Invest 1999;22:811–9.
17. Hansford JR, Mulligan LM. Multiple endocrine neoplasia type 2 and RET: from neoplasia to neurogenesis. J Med Genet 2000;37:817–27.
18. Eng C, Smith DP, Mulligan LM, et al. Point mutation within the tyrosine kinase domain of the RET proto-oncogene in multiple endocrine neoplasia type 2B and related sporadic tumours. Hum Mol Genet 1994;3:237–41.
19. Mulligan LM, Ponder BA. Genetic basis of endocrine disease: multiple endocrine neoplasia type 2. J Clin Endocrinol Metab 1995;80:1989–95.
20. Carlson KM, Dou S, Chi D, et al. Single missense mutation in the tyrosine kinase catalytic domain of the RET protooncogene is associated with multiple endocrine neoplasia type 2B. Proc Natl Acad Sci U S A 1994;91:1579–83.
21. Songyang Z, Carraway KLI, Eck MJ, et al. Catalytic specificity of protein-tyrosine kinases is critical for selective signalling. Nature 1995;373:536–9.
22. Pandit SD, Donis-Keller H, Iwamoto T, Tomich JM, Pike LJ. The multiple endocrine neoplasia type 2B point mutation alters long-term regulation and enhances the transforming capacity of the epidermal growth factor receptor. J Biol Chem 1996;271:5850–8.
23. Smith DP, Houghton C, Ponder BA. Germline mutation of RET codon 883 in two cases of *de novo* MEN 2B. Oncogene 1997;15:1213–7.
24. Gimm O, Marsh DJ, Andrew SD. Germline dinucleotide mutation in codon 883 of the RET proto-oncogene in multiple endocrine neoplasia type 2B without codon 918 mutation. J Clin Endocrinol Metab 1997;82:3902–4.
25. Miyauchi A, Futami H, Hai N, et al. Two germline missense mutations at codons 804 and 806 of the RET proto-oncogene in the same allele in a patient with multiple endocrine neoplasia type 2B without codon 918 mutation. Jpn J Cancer Res 1999;90:1–5.
26. Iwashita T, Murakami H, Kurokawa K, et al. A two-hit model for development of multiple endocrine neoplasia type 2B by RET mutations. Biochem Biophys Res Commun 2000;268:804–8.
27. Menko FH, van Der Luijt RB, de Valk IA, et al. Atypical MEN type 2B associated with two germline RET mutations on the same allele not involving codon 918. J Clin Endocrinol Metab 2002;87:393–7.
28. Bolino A, Schuffenecker I, Luo Y, et al. RET mutations in exons 13 and 14 of FMTC patients. Oncogene 1995;10:2415–9.
29. Stone EA, Sidow A. Physicochemical constraint violation by missense substitutions mediates impairment of protein function and disease severity. Genome Res 2005;15:978–86.
30. Kashuk CS, Stone EA, Grice EA, et al. Phenotype-genotype correlation in Hirschsprung disease is illuminated by comparative analysis of the RET protein sequence. Proc Natl Acad Sci U S A 2005;102:8949–54.
31. Bongarzone I, Monzini N, Borrello MG, et al. Molecular characterization of a thyroid tumor-specific transforming sequence formed by the fusion of ret tyrosine kinase and the regulatory subunit RIα of cyclic AMP-dependent protein kinase A. Mol Cell Biol 1993;13:358–66.
32. Borrello MG, Alberti L, Arighi E, et al. The full oncogenic activity of Ret/ptc2 depends on tyrosine 539, a docking site for phospholipase Cγ. Mol Cell Biol 1996;16:2151–63.
33. Hubbard SR. Crystal structure of the activated insulin receptor tyrosine kinase in complex with peptide substrate and ATP analog. EMBO J 1997;16:5572–81.
34. Kasprzak L, Nolet S, Gaboury L, et al. Familial medullary thyroid carcinoma and prominent corneal nerves associated with the germline V804M and V778I mutations on the same allele of RET. J Med Genet 2001;38:784–7.
35. Bartsch DK, Hasse C, Schug C, Barth P, Rothmund M, Hoppner W. A RET double mutation in the germline of a kindred with FMTC. Exp Clin Endocrinol Diabetes 2000;108:128–32.
36. Carniti C, Perego C, Mondellini P, Pierotti MA, Bongarzone I. PP1 inhibitor induces degradation of RETMEN2A and RETMEN2B oncoproteins through proteosomal targeting. Cancer Res 2003;63:2234–43.
37. van der Geer P, Hunter T, Lindberg RA. Receptor protein-tyrosine kinases and their signal transduction pathways. Annu Rev Cell Biol 1994;10:251–337.
38. Zheng J, Knighton DR, Xuong NH, Taylor SS, Sowadski JM, Ten Eyck LF. Crystal structures of the myristylated catalytic subunit of cAMP-dependent protein kinase reveal open and closed conformations. Protein Sci 1993;2:1559–73.
39. Tsigelny I, Greenberg JP, Cox S, Nichols WL, Taylor SS, Ten Eyck LF. 600 ps molecular dynamics reveals stable substructures and flexible hinge points in cAMP dependent protein kinase. Biopolymers 1999;50:513–24.
40. Scurini C, Quadro L, Fattoruso O, et al. Germline and somatic mutations of the RET proto-oncogene in apparently sporadic medullary thyroid carcinomas. Mol Cell Endocrinol 1998;137:51–7.
41. Uchino S, Noguchi S, Adachi M, et al. Novel point mutations and allele loss at the RET locus in sporadic medullary thyroid carcinomas. Jpn J Cancer Res 1998;89:411–8.
42. Shannon KE, Gimm O, Hinze R, Dralle H, Eng C. Germline V804M mutation in the RET proto-oncogene in two apparently sporadic cases of MTC presenting in the seventh decade of life. J Endocr Genet 1999;1:39–46.
43. Fink M, Weinhusel A, Niederle B, Haas OA. Distinction between sporadic and hereditary medullary thyroid carcinoma (MTC) by mutation analysis of the RET proto-oncogene. Study Group Multiple Endocrine Neoplasia Austria (SMENA). Int J Cancer 1996;69:312–6.
44. Fattoruso O, Quadro L, Libroia A, et al. A GTG to ATG novel point mutation at codon 804 in exon 14 of the RET proto-oncogene in two families affected by familial medullary thyroid carcinoma. Hum Mutat 1998;1:S167–71.
45. Hubbard SR. Autoinhibitory mechanisms in receptor tyrosine kinases. Front Biosci 2002;1:330–40.
46. Moore MJ, Kanter JR, Jones KC, Taylor SS. Phosphorylation of the catalytic subunit of protein kinase A. Autophosphorylation versus phosphorylation by phosphoinositide-dependent kinase-1. J Biol Chem 2002;277:47878–84.
47. Carlomagno F, Vitagliano D, Guida T. The kinase inhibitor PP1 blocks tumorigenesis induced by RET oncogenes. Cancer Res 2002;62:1077–82.
48. Carlomagno F, Vitagliano D, Guida T. ZD6474, an orally available inhibitor of KDR tyrosine kinase activity, efficiently blocks oncogenic RET kinases. Cancer Res 2002;62:7284–90.
49. Karni R, Mizrachi S, Reiss-Sklan E, Gazit A, Livnah O, Levitzki A. The pp60c-Src inhibitor PP1 is non-competitive against ATP. FEBS Lett 2003;537:47–52.
50. Carlomagno F, Santoro M. Identification of RET kinase inhibitors as potential new treatment for sporadic and inherited thyroid cancer. J Chemother 2004;16:S49–51.
51. Niswender CM, Ishihara RW, Judge LM, Zhang C, Shokat KM, McKnight GS. Protein engineering of protein kinase A catalytic subunits results in the acquisition of novel inhibitor sensitivity. J Biol Chem 2002;277:28916–22.
52. Carlomagno F, Santoro M. Receptor tyrosine kinases as targets for anticancer therapeutics. Curr Med Chem 2005;12:1773–81.
53. Sawyers CL. Rational therapeutic intervention in cancer: kinases as drug targets. Curr Opin Genet Dev 2002;12:111–5.
54. Weisberg E, Griffin JD. Resistance to imatinib (Glivec): update on clinical mechanisms. Drug Resist Updat 2003;6:231–8.
55. Specht KM, Shokat KM. The emerging power of chemical genetics. Curr Opin Cell Biol 2002;14:155–9.